Incremental Nonlinear Dynamic Inversion for Quadrotor Control

Eduardo Lima Simões da Silva

November 16, 2015

Abstract

In this extended abstract the research developed on the feasibility of implementation of an Incremental Non-linear Dynamic Inversion (INDI) control for quadrotor control is divided into four main topics. First, a background study on the state of the art for linear and non-linear adaptive controllers is given, to provide a review foundation and to motivate the study of this Incremental controller. Secondly, a detailed study about quadrotor modelling is presented, where an audition to how previous research modelled different quadrotors, leading to a reasoned choice of quadrotor helicopter model. Thirdly, the attitude and position controller are deduced, investigated and implemented in simulation. The attitude controller has an INDI inner loop that aims to cancel the non-linearities and couplings of the system and a linear derivative and proportional outer loop to control the attitude. The position controller uses a similar architecture but also combines a Pseudo Control Hedging Algorithm that aims to increase the performance of the controller by changing the reference provided when certain saturations are reached. Lastly, the results obtained with the implemented controllers are compared with the results from a linear controller (Proportional/Incremental/Derivative) and a NDI controller, developed in a similar simulation in previous work. This comparison is not only performed for usual flight conditions, but also for flight conditions with faults in the actuators, changes of mass and with other different disturbances, where the advantage of the use of an INDI controller is expected to be more evident.

I. Introduction

Quadcopters are nowadays a global phenomenon. They are used in a large number of applications, from mapping to agriculture, through the media industry and other recreational activities. Quadcopters or quadrotor helicopters are also used in more critical applications such as search and rescue, infrastructure inspections or even as a tool in medical emergency. Such critical applications may force the equipment to perform aggressive manoeuvres indoors and outdoors. Increasing the risk of physical damages or other failures to occur. Either while flying over a crowd or while doing a critical task, the robustness and the consistency of the behaviour of a quadrotor is critical to the safety of the bystanders and the equipment itself.

This project consists in the study and application of the previously developed Incremental Nonlinear Dynamic Inversion Control [2, 6, 1, 7] to a quadrotor platform. The goal of this project is to study the specific way failures or time-varying model uncertainties influence the quadrotor behaviour and its control, and how it is possible to use an Incremental Nonlinear dynamic Inversion in the development of a controller.

While performing aggressive manoeuvres a nonlinear controller is essential to allow the quadcopter to have a large flight envelope. For some applications a reliable controller is critical to save lives (as for the TUDelft Ambulance Drone) and avoid damaging equipment or people (as for quadcopters flying over crowds).

Several linear and nonlinear adaptive controllers were developed to solve model uncertainties while performing aggressive manoeuvres, usually by means of an online identification. Adaptive neural networks [4] or adaptive NDI [5] are examples of such controllers.

II. Adopted Model

The Bebop drone quadrotor was divided into four parts: Engine Dynamics, Propellers Model, Quadrotor Dynamics and Quadrotor Kinematics. as seen in the block diagram shown in figure 1. The inertial reference frame (E) was defined as a North-East-Down (NED) where the two first axes (x and y) are aligned with the meridian and parallel lines, respectively, and the last axis (z) is pointing down to the center of the earth. The body reference frame (B) chosen follows the conventional plus configuration, represented in figure 2, with the body axes are aligned with the quadrotor rods. The body reference frame leads to the adoption of equation 1 for the angular dynamics of the quadrotor, where I is the inertia matrix defined in 2 and l is the distance between the center of the propeller and the axis of rotation, that for plus configuration is equal to the size

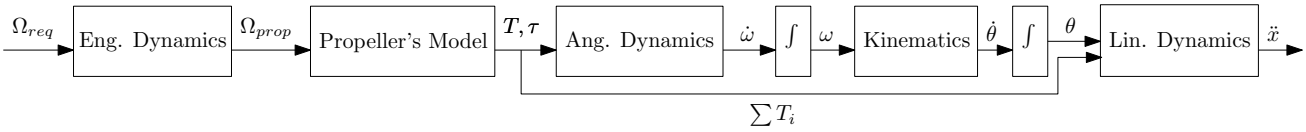

Figure 1: Block diagram of the Quadrotor Model adopted.

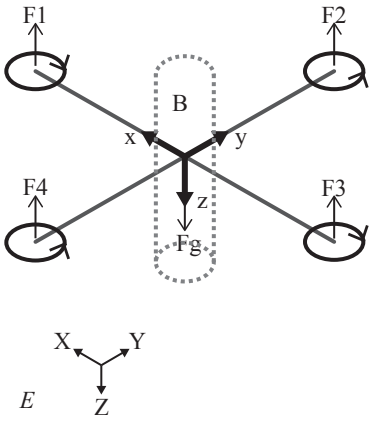

Figure 2: A plus (+) reference frame with the simplified of the quadrotor adopted in grey.

of the rod, and assumed to be 12.6 cm.

$$\begin{bmatrix}\dot{\omega}_1\\ \dot{\omega}_2\\ \dot{\omega}_3\\ F_t\end{bmatrix} = \begin{bmatrix} & I^{-1} & & 0\\ & & & 0\\ & & & 0\\ 0 & 0 & 0 & 1\end{bmatrix}\begin{bmatrix} lF_1 - lF_3\\ -lF_2 + lF_4\\ -\tau_1 + \tau_2 - \tau_3 + \tau_4\\ F_1 + F_2 + F_3 + F_4\end{bmatrix} - \begin{bmatrix} & I^{-1} & & 0\\ & & & 0\\ & & & 0\\ 0 & 0 & 0 & 1\end{bmatrix}\begin{bmatrix}\omega \times I\omega\\ 0\end{bmatrix} \quad (1)$$

Where ω is the angular rate in the body frame, $\dot{\omega}$ is the angular acceleration in the body frame, F_t is the total force produced by all the propellers, F_i is the force produced by rotor i and τ_i is the torque produced by rotor i with $i = 1, ..., 4$.

$$m = 0.4kg, \quad I = \begin{bmatrix}0.00223 & 0 & 0\\ 0 & 0.00299 & 0\\ 0 & 0 & 0.00480\end{bmatrix} kgm^2$$

$$P_{cg} = \begin{bmatrix}-0.001\\ 0\\ 0.007\end{bmatrix} m \quad (2)$$

where m is the total mass of the quadrotor, I is the inertial matrix and P_{cg} is the position of the center of mass. The transformation between between both referential frames can be done by a rotation as: $x_E = Rx_B$ and $x_B = R^{-1}x_E$, where R is defined in 3:

$$R = \begin{bmatrix}c(1)c(3) & -c(1)s(3) + c(3)s(1)s(2) & s(3)s(2) + c(3)s(1)c(2)\\ c(1)s(3) & s(1)s(2)s(3) - c(1)c(2) & -c(1)s(2) + s(3)s(1)c(2)\\ -s(1) & c(1)s(2) & c(1)c(2)\end{bmatrix} \quad (3)$$

With the Euler angles $\theta = (1, 2, 3) = (\theta_1, \theta_2, \theta_3)$ as pitch, roll and yaw angles, and c, s represent the cosine and sine respectively.
The engined dynamics has a very important role on the quadrotor performance and was considered as a first order filter with a cutting frequency of around $50Hz$:

$$H(s) = \frac{1}{1 + T.s} \quad (4)$$

The propellers model follows the quadratic relation between the propeller rotation speed and the Thrust/Torque produced:

$$T_i(\Omega) = K_{T_2}\Omega_i^2 + K_{T_1}\Omega_i + K_{T_0} \quad (5)$$

$$\tau_i(\Omega) = T_i K_\tau \quad (6)$$

with the coefficients for this relation (K_{T_2}, K_{T_1}, K_{T_0} and K_τ) found with a parameter estimation described in section III, as in [5]. The kinematics equation, uses the Euler angles, and determines the relation between the angular body rates and the Euler rates, as defined in equation 7. This component mainly aims to define the relation between the movement in the body reference frame to the inertial reference frame, obtaining the Euler rates from the body rates.

$$\dot{\theta}_{Earth} = J(\theta)\omega_{body} \quad (7)$$

$$(8)$$

Where J can be defined as:

$$J = \begin{bmatrix}1 & \sin(\theta_1)\tan(\theta_2) & \cos(\theta_1)\tan(\theta_2)\\ 0 & \cos(\theta_1) & -\sin(\theta_1)\\ 0 & \frac{\sin(\theta_1)}{\cos(\theta_2)} & \frac{\cos(\theta_1)}{\cos(\theta_2)}\end{bmatrix} \quad (9)$$

It would be relatively easy to use a standard quaternion kinematics equation, this would produce the clear advantage of the elimination of the singularity around $\theta_2 = \pm 90^o$.
The dynamics of the quadrotor can be described as:

$$F = m\dot{V} \quad (10)$$

$$M = I\dot{\omega}_b + \omega_b \times I\omega_b \quad (11)$$

Where the momentum equation was already described

in 1, and the linear dynamics can be described in:

$$\begin{bmatrix} \ddot{x} \\ \ddot{y} \\ \ddot{z} \end{bmatrix}_E = \frac{1}{m} R(\theta) \left(\begin{bmatrix} 0 \\ 0 \\ -F_T \end{bmatrix} - F_{drag} \right]_B + \begin{bmatrix} 0 \\ 0 \\ g \end{bmatrix}_E \quad (12)$$

In equation 12, F_T represents the total force applied by the actuators, F_{drag} is the aerodynamic drag described in 13, g is the acceleration of gravity, usually defined as $9.80665 m/s^2$, $[\ddot{x} \quad \ddot{y} \quad \ddot{z}]_E^T$ is the linear acceleration vector defined in the NED frame, $R(\theta)$ is the rotational matrix shown in equation 3, $m = 0.400kg$ is the quadrotor mass and F_T is the sum of the thrust produced by all the motors.

$$F_{drag} = \frac{K_{drag} \rho A |V| V}{2} \quad (13)$$

The choice of the drag coefficient is intimately related with the shape of the quadrotor, the total area perpendicular to the speed and square of the relative air speed. Here for the y and z body axes a coefficient (here defined as K_{drag}) usually associated with a cylinder was assumed, while for the aerodynamic drag along x a more rounded shape was assumed. These assumptions make this drag model very rough.

I. Simulation model

In the Bebop Drone, there are three main sensors available that are relevant for the implementation: a 3-axes rate gyroscope, a 3-axes accelerometer and a motor rotation speed sensor. Additionally, there are other sensors available that won't be taken into consideration during the simulation but that are used in the system. This simulation runs with a sampling frequency of $512Hz$ which is the sampling frequency available on-board of the Bebop Drone. Furthermore, this model also includes the addition of signal noise in the three measurements considered, as well as an atmospheric disturbance input simulating wind.

III. Identification and Parameter estimation

The thrust coefficients parameter identification was performed with a static test that aimed to identify the relation between the propellers rotational speed with the thrust produced by the four propellers. To perform this test, the quadrotor was firmly assembled upside down on a scale, with approximately $40cm$ separation between the scale and the propellers to minimize the effect of the ground on the measurements. An increasing sequence of propellers speed was given to the quadrotor while the values of the weight presented in the scale were registered.

With the rotational propeller speed and thrust data it was possible to perform a quadratic regression to obtain the parameters for the the second order degree polynomial of the form $T(\Omega) = K_{T_2}\Omega^2 + K_{T_1}\Omega + K_{T_0}$. In figure 4 it is possible to visualize the obtained quadratic line fitted to the available data. This quadratic regression resulted in the values $K_{T_2} = 7.088706 \times 10^{-05} Ns^2 \quad K_{T_1} = -0.002282787 Ns \quad K_{T_0} = 0.08001036 N$. During the experiment the maximum rotation speed was requested to the engines, approximately $180Hz$, this was considered, the maximum achievable propellers speed. This constraint was taken into consideration during the implementation of the simulation and resulted in the maximum thrust of approximately $1.96N$ per rotor.

IV. Fundamentals of INDI

A critical advantage of INDI is the fact that only a small portion of the model (control derivatives)[6] is required for the design of the model, and even this small portion does not critically affect the control performance, reducing the importance of possible discrepancies between the real model and the identified one. The Incremental Nonlinear Dynamic Inversion (INDI) controller can be derived from a general nonlinear system:

$$\dot{x} = f(x, u) \quad (14)$$

Taking a Taylor series expansion the system can be linearised at the current time step:

$$\begin{aligned} \dot{x} &\simeq f(x_0, u_0) + \left. \frac{\partial f(x,u)}{\partial x} \right|_{x=x_0, u=u_0} (x - x_0) \\ &+ \left. \frac{\partial f(x,u)}{\partial u} \right|_{x=x_0, u=u_0} (u - u_0) \\ &\simeq \dot{x}_0 + F(x_0, u_0)(x - x_0) + G(x_0, u_0)(u - u_0) \end{aligned} \quad (15)$$

Simplifying equation 15 by the application of the time scale principle when the system sample rate is considered to be high, the variation $x - x_0$ can be neglected when compared with the rest of the system, resulting in the following by using the incremental form:

$$\dot{x} \simeq \dot{x}_0 + G(x_0, u_0)\Delta u \quad (16)$$

An NDI controller can then be designed in the incremental form by solving in relation to Δu equation 16, and where $\dot{x}$ is assumed to be the virtual control variable ν:

$$\Delta u = G(x_0, u_0)^{-1}(\nu - \dot{x}_0) \quad (17)$$

Where $\dot{x}_0$ is assumed to be measurable and the control matrix $G(x_0, u_0)$ contains the relation to the specified

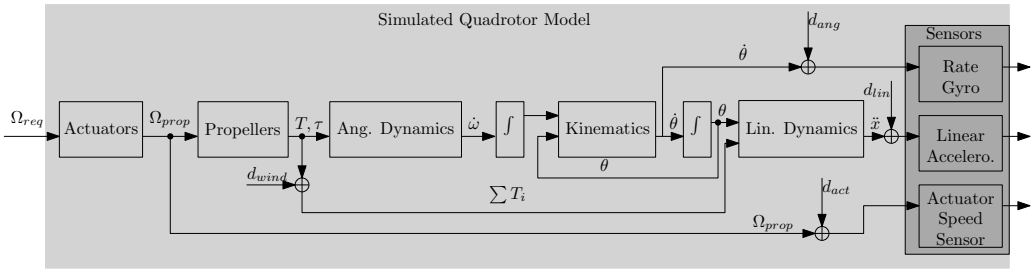

Figure 3: Block diagram of the Quadrotor Model implemented in simulink.

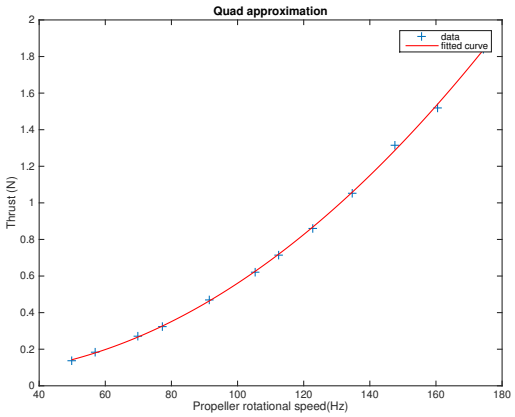

Figure 4: Quadratic regression line fit and data

controller, the real control inputs need to be updated by increments as $u_{new} = u_{current} + \Delta u$. When applying the resulting controller to the original system, eq. 16, the following is obtained:

$$\begin{aligned} \dot{x} &\simeq \dot{x}_0 + G(x_0, u_0)G(x_0, u_0)^{-1}(\nu - \dot{x}_0) \\ &\simeq \nu \end{aligned} \tag{18}$$

In figure 5 the usual architecture that was explained in this section is presented in a block diagram, shown in figure 5. The advantages of INDI are clear in equation

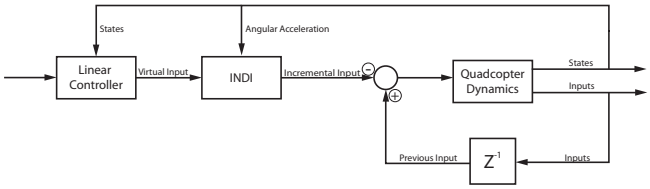

Figure 5: General block diagram of an INDI controller.

17, by using the angular acceleration measurements all uncertainties that do not depend on the input are eliminated. The dynamic inversion is considerably simplified by including in the measurements the uncertain components. Recalling the system in its incremental form presented in equation 16, it is possible to rewrite it when uncertainties exist in both the inertia and control matrices in equation 19.

$$\dot{x} = \dot{x}_0 + G(x_0, u_0)\Delta u + \Delta G(x)\Delta u \tag{19}$$

Applying the INDI developed for the incremental model to the uncertain system shown in equation 19, results in the closed loop system:

$$\begin{aligned} \dot{x} &= \dot{x}_0 + G(x_0, u_0)G(x_0, u_0)^{-1}[\nu - \dot{x}_0] \\ &\quad + \Delta G(x)G(x_0, u_0)^{-1}[\nu - \dot{x}_0] \\ &= \dot{x}_0 + I[\nu - \dot{x}_0] + \Delta G(x)G(x_0, u_0)^{-1}[\nu - \dot{x}_0] \\ &= \nu + \Delta G(x)G(x_0, u_0)^{-1}\nu \\ &\quad - \Delta G(x)G(x_0, u_0)^{-1}\dot{x}_0 \end{aligned} \tag{20}$$

Assuming that the sensor provides ideal measurements, the difference between new and current angular acceleration is very small for a high sample rate, resulting in $\dot{x}_0 \simeq \dot{x}$, this allows to rewrite equation 20 as:

$$\begin{aligned} \dot{x} &= \nu + \Delta G(x)G(x, u_0)^{-1}\nu \\ &\quad -\Delta G(x)G(x, u_0)^{-1}\dot{x} \end{aligned} \tag{21}$$

Equation 21 can be rearranged into equation 22 in order to conclude that $\dot{x} = \nu$.

$$\begin{aligned} \dot{x} &= \left[I + \Delta G(x)G(x, u_0)^{-1}\right]^{-1} \\ &\quad \left[I + \Delta G(x)G(x, u_0)^{-1}\right]\nu \\ &= \nu \end{aligned} \tag{22}$$

This is an interesting result that shows that even with uncertainties in the control matrix, with a high sample rate, the INDI controller is robust.

V. Sensor Noise, Delay and Sampling Frequency

The angular acceleration measurements are a critical issue in the design of an INDI controller. Usually, the angular acceleration is not measured directly, its sensors are not widely available, specially for small

unmaned aircrafts.
This results in the need of using indirectly obtained angular accelerations. The process of differentiation of the velocity amplifies the noise of the measurement, resulting in an angular acceleration measurement with amplified noise[3]. Consequentially, this indirectly obtained angular acceleration measurement does not agree with the assumptions of perfect measurements and ideal sensors made until now.
As the INDI controller decouples the states of the system it is possible to address the filtering problem by considering simple signal filtering. A compromise between delay and noise with a low pass filter needs to be found. The development of INDI also assumed that the sampling rate was high in order to allow some simplifications to take place. The model implemented is inspired on a quadrotor that has a sampling rate of $512Hz$, which was considered high and allowed for the assumptions to be considered valid.

VI. Attitude Controller

From now on we will take our state as x_{ang} that includes θ and ω as can be seen in 23, where $\theta_{1,2,3}$ are the Euler angles (pitch, roll and yaw) and $\omega_{1,2,3}$ are the body rotational speed around x_{ang}, y_{ang} and z_{ang} body axes.

$$x_{ang} = \begin{bmatrix} \theta \\ \omega \end{bmatrix} = \begin{bmatrix} \theta_1 \\ \theta_2 \\ \theta_3 \\ \omega_1 \\ \omega_2 \\ \omega_3 \end{bmatrix} \quad u = \begin{bmatrix} \Omega_1 \\ \Omega_2 \\ \Omega_3 \\ \Omega_4 \end{bmatrix} \tag{23}$$

Where Ω, represents the rotational speed of the propellers of the quadrotor.
Since the control variable that we are aiming to control is the Euler angles, we can define θ as our output variable and later as control variable, as seen in 24.

$$y = \theta = Hx_{ang} = \begin{bmatrix} I_{3\times3} & 0_{3\times3} \end{bmatrix} x_{ang} \tag{24}$$

I. INDI Loop

The goal of the attitude loop is to control the Euler angles. The direct relation between input and output variables was determined by executing the second order derivative of the control variable vector, as the first order time derivative of the control variable vector does not contain the control input u, as can be seen:

$$\frac{dy}{dt} = \frac{dHx_{ang}}{dt} = H\dot{x_{ang}} = H \begin{bmatrix} J(\theta)\omega \\ \dot{\omega} \end{bmatrix} = J(\theta)\omega \tag{25}$$

where a short notation was used: $c()$, $s()$ and $t()$ representing $\cos()$, $\sin()$ and $\tan()$ respectively:

$$\frac{d^2y}{dt^2} = \frac{d(J(\theta)\omega)}{dt} =$$
$$= \frac{d}{dx_{ang}} \left(\begin{bmatrix} 1 & s(\theta_1)t(\theta_2) & c(\theta_1)t(\theta_2) \\ 0 & c(\theta_1) & -s(\theta_1) \\ 0 & \frac{s(\theta_1)}{c(\theta_2)} & \frac{c(\theta_1)}{c(\theta_2)} \end{bmatrix} \begin{bmatrix} \omega_1 \\ \omega_2 \\ \omega_3 \end{bmatrix} \right) \dot{x}_{ang} \tag{26}$$

It is then clear that in this case the input explicitly appears in the expression. From this point it is possible to deduce the INDI controller for the complete system by performing a Taylor expansion in the current time step. This expansion will provide the linearised relation between the speed of the propellers and the Euler angles.

$$\ddot{y} = f(x_{ang}, u) \tag{27}$$
$$\ddot{y} \approx f(x_{ang_0}, u_0) + \left.\frac{\partial f(x_{ang}, u)}{\partial x_{ang}}\right|_{x_{ang_0}, u_0} (x_{ang} - x_{ang_0}) +$$
$$+ \left.\frac{\partial f(x_{ang}, u)}{\partial u}\right|_{x_{ang_0}, u_0} (u - u_0) \tag{28}$$

The linearisation shown in 28, assumes $f(x_{ang_0}, u_0) = \ddot{x}_{ang_0}$ as the angular acceleration measurement in the previous time step. With a very small sampling time, and considering that the actuator dynamics is faster than the other dynamics of the system, it is possible to assume that $(x_{ang} - x_{ang_0}) \approx 0$ when compared with $(u - u_0)$. The assumption that the actuator dynamics is faster than the system dynamics is quite bold in a quadrotor system, especially because the quadrotor system dynamics is primarily dependent on the actuators dynamics. The simplified expression that will be later used to obtain the control law can be seen as:

$$\ddot{y} \simeq \ddot{y}_0 + G(x_{ang_0}, u_0)\Delta u \tag{29}$$

where matrix $G(x_{ang_0}, u_0)$ is simply the derivative in order of the control inputs of the system, resulting in:

$$G(x_{ang_0}, u_0) =$$
$$= J(\theta) \left[I \begin{bmatrix} & & 0_{3\times4} & \\ r\frac{\partial F_1}{\partial \Omega_1} & 0 & -r\frac{\partial F_3}{\partial \Omega_3} & 0 \\ 0 & -r\frac{\partial F_2}{\partial \Omega_2} & 0 & r\frac{\partial F_4}{\partial \Omega_4} \\ -K_\tau \frac{\partial F_1}{\partial \Omega_1} & K_\tau \frac{\partial F_2}{\partial \Omega_2} & -K_\tau \frac{\partial F_3}{\partial \Omega_3} & K_\tau \frac{\partial F_4}{\partial \Omega_4} \end{bmatrix} \right] \Bigg|_{\Omega_i = \Omega_{i_0}} \tag{30}$$

Where $\frac{\partial F_i}{\partial \Omega_i} = (2K_{t_2}\Omega_i + K_{t_2})$, to complete the deduction of the control law from equation 29, one just has to solve in order of the incremental input. One can then obtain the input for the system with the simple relation $\Delta u = (u - u_0)$, where u_0 is the previous input. The state that includes the control of the total force produced by the system was not yet considered. This means that the control law will have to consider T_F as a control variable. Resulting in a new control law that

was obtained from:

$$\begin{bmatrix}\dot{\omega}_1\\ \dot{\omega}_2\\ \dot{\omega}_3\\ F_T\end{bmatrix} = I_{quad}^{-1}\begin{bmatrix}lF_1 - lF_3\\ lF_2 - lF_4\\ -\tau_1+\tau_2-\tau_3+\tau_4\\ F_1+F_2+F_3+F_4\end{bmatrix} - I_{quad}^{-1}\begin{bmatrix}\omega \times I\omega\\ 0_{1\times 1}\end{bmatrix} \quad (31)$$

where I_{quad} is a newly defined 4×4 matrix, as seen in 32.

$$I_{quad} = \begin{bmatrix}I_{xx} & 0 & 0 & 0\\ 0 & I_{yy} & 0 & 0\\ 0 & 0 & I_{zz} & 0\\ 0 & 0 & 0 & 1\end{bmatrix} \quad (32)$$

For implementation purposes this control change was implemented by simply changing the previously mentioned control law 29 in matrix G to also consider the recent addition. This way the new control law will be the same:

$$\Delta u = G_{quad}(x_{ang_0}, u_0)^{-1}(cv_{quad} - \dot{x}_{0_{quad}}) \quad (33)$$

where $cv_{quad} = [\ddot{\theta}_{1\times 3} \quad F_T]^T$ is the virtual control vector and $\dot{x}_{0_{quad}} = [\ddot{\theta}_{0_{1\times 3}} \quad F_{T_0}]^T$ is the measurement of the angular acceleration and F_T. In this last measurement, T_{F_0} is not obtained directly but relies on the model that relates the propeller speed to the thrust produced. And the new matrix $G_{quad}(x_{ang_0}, u_0)$ is defined as seen in 34, with $G_{force}(u_0) = [2K_{t_2}\Omega_{1_0} + K_{t_1} \quad 2K_{t_2}\Omega_{2_0} + K_{t_1} \quad 2K_{t_2}\Omega_{3_0} + K_{t_1} \quad 2K_{t_2}\Omega_{4_0} + K_{t_1}]$.

$$G_{quad}(x_{ang_0}, u_0) = \begin{bmatrix}G(x_{ang_0}, u_0)\\ G_{force}(u_0)\end{bmatrix} \quad (34)$$

The controller obtained is therefore a non-linear controller that is slightly less dependent on the model, but that is built upon sound angular acceleration measurements that cannot be obtained directly. Even though the controller does not depend on part of the model, it is verifiable that the part of the controller that is neglected only slightly influences the quadrotor behaviour and therefore the advantage gained by disregarding the slower dynamics of the model is not critically meaningful.

II. Attitude Loop

With the correct cancelling of the non-linearities and the possible decoupling between states, it is feasible to implement two additional linear proportional loops to control the Euler rates and the Euler angles sequentially. The overall attitude controller block diagram can be visualized in figure 6. As it is noticeable in figure 7, the total force does not require any additional loop to be controlled. The gains for the proportional loop where chosen sequentially, first tuning the gain

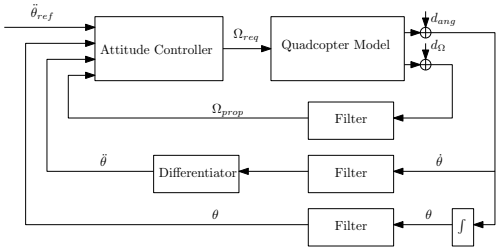

Figure 6: Block diagram of the attitude controller with filters.

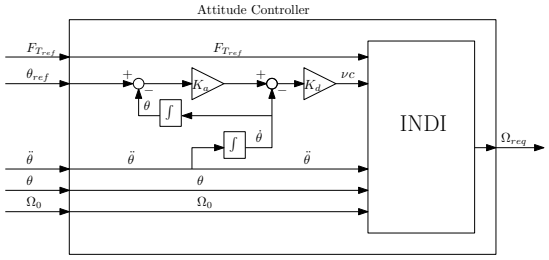

Figure 7: Block diagram of the attitude controller detail.

for a Euler rate controller and only afterwards the second loop was implemented, followed by the tuning of the second gain related with the attitude controller. The filters chosen had a cutting frequency of $50Hz$ and a damping ratio of 5, as explained above these parameters were shared among all the filters.

III. Results

With the controller implemented the doublet response for a Euler angle reference is shown in figure 8.

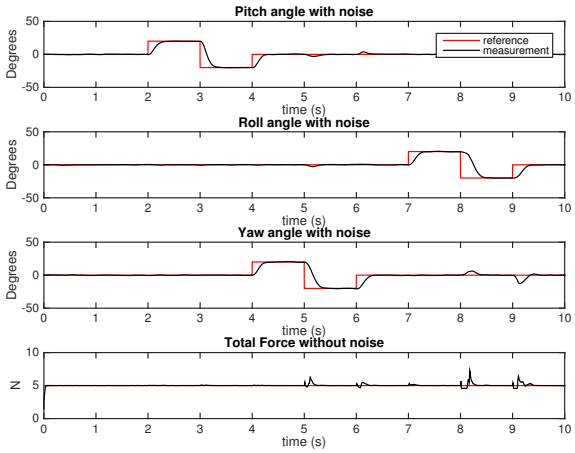

Figure 8: Attitude response to a doublet on the attitude reference.

When requesting very steep pitch or roll angles it is clear that some coupling occurs between the states, as

for example near second 4. In this situation, the noise and delay are not a critical factor. The reason behind the coupling seen in figure 8 is actuators saturation.

VII. Position Controller

The proposed position controller follows a similar idea as the one developed for the attitude control. The first control layer will make use of the Incremental Non-linear Dynamic Inversion technique, this time to cancel the non-linearities associated to the linear dynamics system. This proposed controller also includes a Pseudo Control Hedging to shape the input requested to the controller, taking into consideration the limitations of the system.
It is possible to notice a direct relation between both the Euler angles in matrix R and F_T and the angular accelerations that are the states that need to be controlled at this stage. The virtual control variables chosen for the position INDI controller are defined as ν in 35 and include the linear accelerations and the input of the system will be the pitch and roll angle, that together compose the tilt angle, and the total force but does not include the yaw angle.

$$\nu = \begin{bmatrix} \ddot{x} \\ \ddot{y} \\ \ddot{z} \end{bmatrix}_E \qquad U = \begin{bmatrix} \theta_1 \\ \theta_2 \\ FT \end{bmatrix} \tag{35}$$

The approximated system, after performing the Taylor expansion and disregarding the slower dynamics of the system, will result in the system presented in:

$$\nu = \ddot{x}_0 + G_{outer}\Delta U \tag{36}$$

Where matrix G_{outer} can be defined as the derivative in order to the input variables, θ_1 and θ_2 and TF as:

$$G_{outer} = \begin{bmatrix} a & b & d \\ e & f & h \\ k & l & o \end{bmatrix} \tag{37}$$

with each element specified ahead due to space management issues:

$$\begin{aligned}
a &= F_{T_0}(\cos(\theta_1)\cos(\theta_2)\cos(\theta_3)) \\
b &= F_{T_0}(-\sin(\theta_2)\sin(\theta_1)\cos(\theta_3) + \cos(\theta_2)\sin(\theta_3)) \\
d &= \sin(\theta_1)\cos(\theta_2)\cos(\theta_3) + \sin(\theta_2)\sin(\theta_3); \\
e &= F_{T_0}(\cos(\theta_2)\sin(\theta_3)\cos(\theta_1)) \\
f &= F_{T_0}(-\sin(\theta_2)\sin(\theta_1)\sin(\theta_3) - \cos(\theta_2)\cos(\theta_3)) \\
h &= -\cos(\theta_3)\sin(\theta_2) + \sin(\theta_3)\sin(\theta_1)\cos(\theta_2) \\
k &= F_{T_0}\cos(\theta_2)\sin(\theta_1) \\
l &= F_{T_0}(-\sin(\theta_2)\cos(\theta_1)) \\
o &= \cos(\theta_1)\cos(\theta_2)
\end{aligned}$$

The control law obtained by solving to the incremental input is partially dependent on the defined model, but does not depend neither on the earth acceleration nor the aerodynamic drag:

$$\Delta U = G_{outer}^{-1}(\nu - \ddot{V}_{earth}) \tag{38}$$

$$U_{current} = U_{previous} + \Delta U \tag{39}$$

I. Results

A doublet response for a reference of linear accelerations of the system is presented in figure 9, where it is possible to verify a very satisfactory results that shows us that indeed the non-linearities of the system are correctly cancelled. There is very clear couplings between the horizontal accelerations and the vertical accelerations. The couplings mentioned before can be

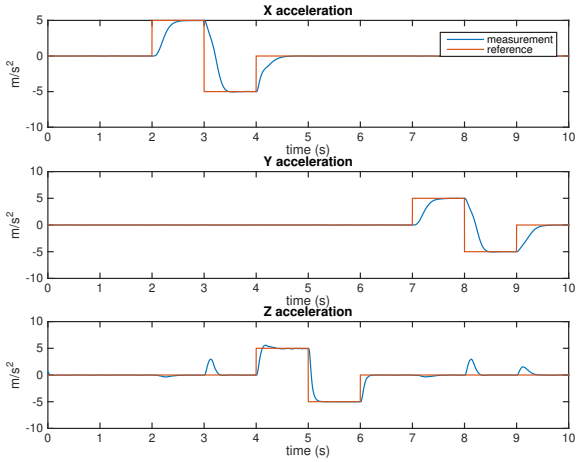

Figure 9: Linear acceleration response for a doublet in the linear acceleration reference.

traced back to the angular references given from the outer loop to the attitude controller. The attitude angles required to achieve a requested acceleration are very steep and therefore the maximum thrust is not enough to maintain the vertical acceleration to the referenced value. This can be verified in figure 10, where the attitude requested by the outer loop is shown as a reference with the attitude response.

II. Pseudo Control Hedging (PCH)

Due to the incremental nature of the controller and the two additional linear PD an P gains it is possible for the controller to request a roll or pitch angle bigger than 90^o . For this reason a saturation of $\pm 80^o$ was included in the reference provided for the pitch and roll angle. The reach of the saturations might affect controllability because discontinuities violate the dynamic inversion requirements, reinforcing the need to find a policy to avoid saturations.

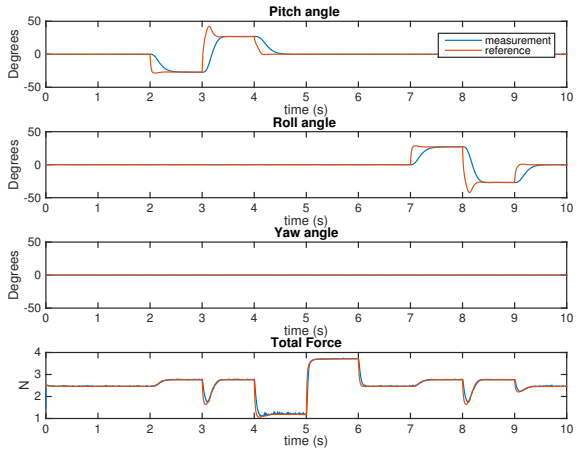

Figure 10: Attitude requested from the outer for the inner loop, and the attitude response

PCH modifies the virtual control, providing a pre-adaptation of the control reference before it is provided to the INDI controller. PCH can be divided into two main parts, a part that includes the reference model (RM), a first order filter that will cut-off frequencies that are physically infeasible, as seen in the block diagram presented in figure 11. The second part of the PCH

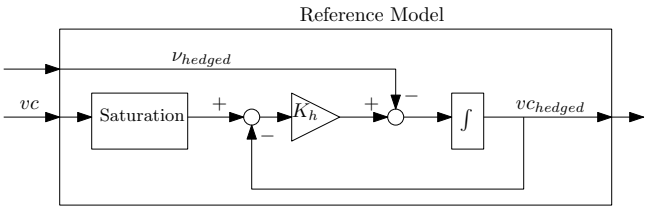

Figure 11: Reference model block diagram.

algorithm consists on the estimation of how much the plant did not move due to the limitations of the attitude dynamics, or as seen from the outer loop, the actuators that are not considered in the controller. This estimation of the PCH will limit the requested virtual control in the reference model, once the saturations no longer occur the attenuation on the commands is no longer active. For the INDI controller the PCH assumes the form of ν_{hedged} as seen in equation 40, depending on the same matrix as the outer INDI control loop, where the virtual control is the linear acceleration and the inputs are the Euler angles.

$$\begin{aligned} &\nu_{hedged} = \nu - \hat{\nu} = \\ &= [\dot{x}_0 + g(x_0)(U_{req} - U_0)] - [\dot{x}_0 + g(x_0)(U - U_0)] \\ &= g(x_0)(U_{req} - U) \end{aligned} \tag{40}$$

In the block diagram presented in figure 12 it is possible to verify the framework were the PCH algorithm is included, receiving both the attitude angles required and the current angular state of the system, and providing the ν_{hedged} to be considered in the reference model.

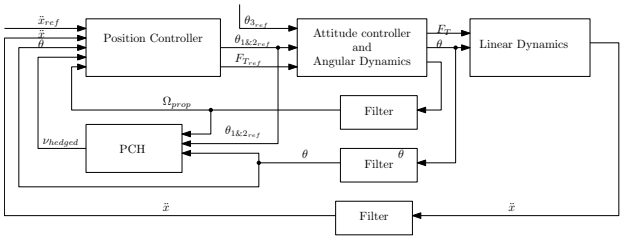

Figure 12: Block diagram including the Pseudo Control Hedging blocks.

III. Position controller

With the INDI controller of the outer loop it is possible to control the linear acceleration of the quadrotor. By adding two linear outer loops to control the velocity and position, results in the controller shown in the block diagram presented in figure 13. The linear gains

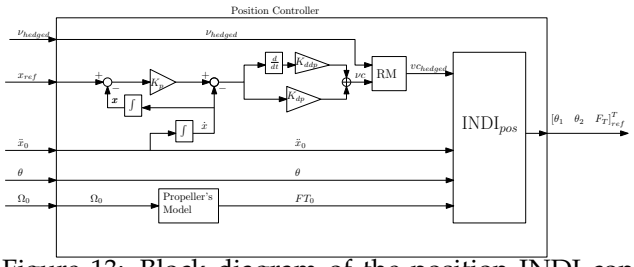

Figure 13: Block diagram of the position INDI controller.

shown were obtained, once again by first analysing the speed controller and tuning its gains. And only after that addressing the proportional gain for the position error.

IV. Results

After implementing the two additional outer loops that aim to sequentially control the linear speed and the linear position it is possible to obtain a position response while providing a position reference, as seen in figure 14. The position response obtained is quite satisfiable as allows the quadrotor to quickly change its position. The coupling between the horizontal and vertical movement is very noticeable in figure 14 where the altitude decreases around 1 meter when the quadrotor changes its position from $x = 0m$ to $x = 10m$. Again due to the very steep roll and pitch angles required to the system.

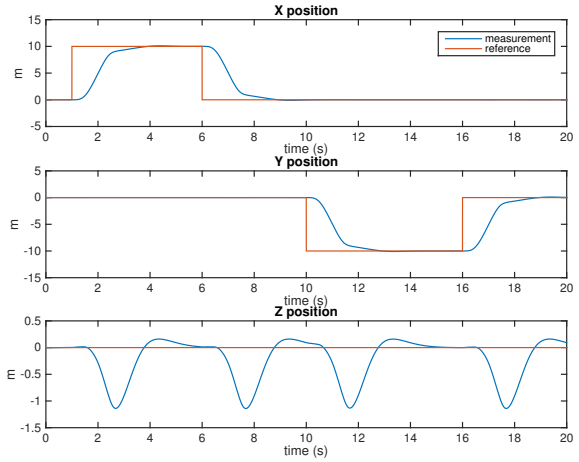

Figure 14: Position response of the quadrotor to the reference provided.

VIII. Results and Comparisons

The position controller will be qualitatively compared with two other controllers implemented in literature. In table 2 a summary of the simulation results presented in **??** and the simulation results obtained by the INDI controller implemented are shown. This simulation consisted in a position step response, with a reference change of 2 meters in the horizontal axes. This results, for the INDI controller, on an temporary increase of the tilt angle to 30º.

Controller	I. Pos.(m)	F. Pos.(m)	Rising Time(s)
PID [8]	$[0,0,2]$	$[2,2,2]$	≈ 2.5
NDI [8]	$[0,0,2]$	$[2,2,2]$	≈ 2
INDI	$[0,0,2]$	$[2,2,2]$	2.25

Table 1: Position Tracking performance comparison table.

It is not possible to clearly show the benefits of using a non-linear controller. Because the task executed is not the ideal, as it does not require for large attitude angles to be maintained for a large period of time.

IX. Robustness Tests

Aggressive manoeuvring and fault tolerance are not usually studied in simultaneous. The literature [5] focusses in aggressive manoeuvring while [8] the focus is the study of the influence of actuator faults in the performance of the system. The second reference will now serve as a reference for the influence of actuator faults in controller performance.

I. Actuator effectiveness

The most influential components of the quadrotor model are its actuators, therefore it is important to study the influence actuator faults in the performance. While executing the same task, one of the rotors suffers a decrease of its effectiveness around second 2. The results of these simulations, are presented in figure 15 where it is possible to verify the increasing effects of the actuator effectiveness loss in the maximum deviation from the position hold reference and the increased difficulty to perform the tracking task. In figure 15

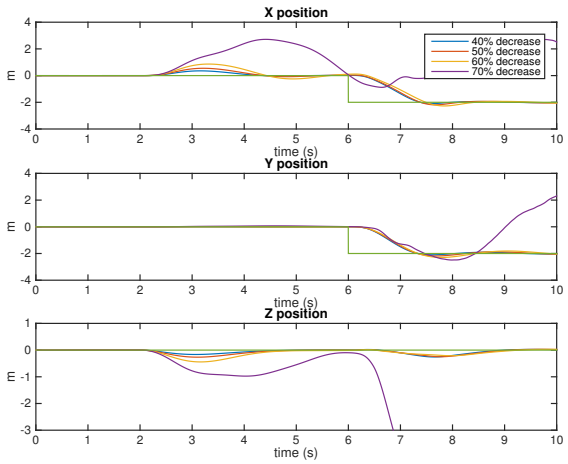

Figure 15: Control performance comparison between NDI and INDI attitude controllers.

it is possible to verify the different effects of different changes on the actuator effectiveness.

Controllers	I. Pos.(m)	Final Pos.(m)	Rising Time(s)
PID [8]	$[0,0,2]$	NA	inf.
NDI [8]	$[0,0,2]$	NA	inf.
PID* [8]	$[0,0,2]$	$[2,2,2]$	≈ 2.5
NDI* [8]	$[0,0,2]$	$[2,2,2]$	≈ 2
INDI	$[0,0,2]$	$[2,2,2]$	2.25

Table 2: Control performance comparison table with a 50% fault in engine 1, at $t = 2s$. *-indicates that a limitation of the reference provided to the system was included.

As seen in table 2 both PID and NDI controllers benefit from the limitations in the attitude reference, limiting the aggressive manoeuvres to keep flying. The INDI controller, also as seen in figure 15, is able to maintain the quadrotor flying while performing some degree of aggressive manoeuvres, being dependent and limited by the actuator saturations.

II. Mass Variations

Mass changes are very common to occur in a very wide range of applications. All require a controller that is able to sustain mass changes and continues to operate normally, making the study of how a mass variation influences the performance of the system without any tuning interesting and useful.
The same task was executed when a certain mass was added to the system in its CG. Figure 16 shows the results for different mass additions to the CG, here displayed in percentage of the initial quadrotor total mass.
The most noticeable effects are verified in the altitude

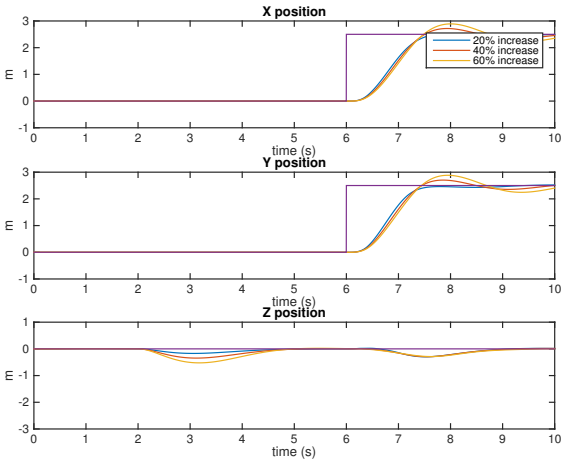

Figure 16: Comparison between different mass increases at second 2, when the different loads are applied directly in the center of gravity.

change when the load is applied and in the increased number of oscillations when the step input is provided to the system and the increased loss of altitude when the quadrotor aims to follow the horizontal position reference.

X. Conclusions

The main goal of this project was to achieve a complete quadrotor controller with the use INDI control theory that showed improvements with the control of a time varying quadrotor model. This goal can be considered convincingly achieved specially after comparing the results obtained with the performance of other controllers in the same situations.
Overall the research developed can be considered successful as the majority of the research questions were answered with conclusions founded on the research. The robustness tests and the comparisons with other controllers also implemented in simulation in previous research allowed to take conclusions about the advantages and drawbacks of the use of an Incremental Non-Linear Dynamic Inversion in a quadrotor system. There are a lot of subjects related with this topic that are currently being investigated, making this a quite interesting, innovative and dynamic topic, and there is still some improvements and future work to be developed in this topic, with the goal of making quadrotors a more reliable, versatile, safe and robust tool for the increasing number of their critical applications.
These tasks include the use of quaternions in the kinematics equation, improve the robustness by using an online identification method and improve actuator saturation management.

References

[1] Paul Acquatella, Wouter Falkena, Erik-Jan van Kampen, and Qi Ping Chu. Robust nonlinear spacecraft attitude control using incremental nonlinear dynamic inversion. In *Proceedings of the AIAA Guidance, Navigation, and Control Conference and Exhibit*, 2012.

[2] Gabriele Di Francesco, Egidio D Amato, and Massimiliano Mattei. Incremental Nonlinear Dynamic Inversion and Control Allocation for a Tilt Rotor UAV. In *AIAA Guidance Navigation and Control Conference*, National Harbor, Maryland, 2014.

[3] Francesco Gianfelici. A novel technique for indirect angular acceleration measurement. *Proceedings of the 2005 IEEE International Conference on Computational Intelligence for Measurement Systems and Applications, CIMSA 2005*, 2005(July):120–123, 2005.

[4] E N Johnson and S Kannan. Adaptive flight control for an autonomous unmanned helicopter. *Proceedings of the 2002 AIAA Guidance, Navigation and Control Conference*, (August), 2002.

[5] C Poppe, E Van Kampen, C De Wagter, C C De Visser, and Q P Chu. Aggressive Quadrotor Maneuvering by Using Nonlinear Dynamic Inversion with Pseudo-Control Hedging and Flight Mode Transition. Master's thesis, Delft University of Technology, 2014.

[6] S. Sieberling, Q. P. Chu, and J. a. Mulder. Robust Flight Control Using Incremental Nonlinear Dynamic Inversion and Angular Acceleration Prediction. *Journal of Guidance, Control, and Dynamics*, 33(6):1732–1742, 2010.

[7] Pedro Valério Menino Simplício. Helicopter Nonlinear Flight Control using Incremental Nonlinear Dynamic Inversion. Master's thesis, Delft University of Technology, 2011.

[8] A.R.J. Stolk. Quadrotor Fault Tolerant Control. Master's thesis, Delft University of Technology, 2015.